International Journal of Mechanical, Industrial and Aerospace Sciences
ISSN: 2517-9950
Vol:11, No:4, 2017

Gyrotactic Microorganisms Mixed Convection Nanofluid Flow along an Isothermal Vertical Wedge in Porous Media

A. Mahdy

***Abstract*—**The main objective of the present article is to explore the state of mixed convection nanofluid flow of gyrotactic microorganisms from an isothermal vertical wedge in porous medium. In our pioneering investigation, the easiest possible boundary conditions have been employed, in other words when the temperature, the nanofluid and motile microorganisms' density have been considered to be constant on the wedge wall. Adding motile microorganisms to the nanofluid tends to enhance microscale mixing, mass transfer, and improve the nanofluid stability. Upon the Oberbeck–Boussinesq approximation and non-similarity transmutation, the paradigm of nonlinear equations are obtained and tackled numerically by using the R.K. Gill and shooting methods to obtain the dimensionless velocity, temperature, nanoparticle concentration and motile microorganisms density together with the reduced Sherwood, Nusselt, and numbers. Bioconvection parameters have strong effect upon the motile microorganism, heat, and volume fraction of nanoparticle transport rates. In the case when bioconvection is neglected, the obtained computations were found in very good agreement with the previous published data.

***Keywords*—**Bioconvection, wedge, gyrotactic microorganisms, porous media, nanofluid, mixed.

I. Introduction

SEVERAL types of fluids are poor heat transfer, such as water, ethylene glycol and mineral oils. Because the thermal conductivity of such fluids has an important role on the heat transfer, namely between the heat transfer medium and the heat transfer plate; numerous methods are proposed to ameliorate the thermal conductivity of these fluids by annotating nano/micro-sized particle materials in liquids (Nanofluid). Namely, nanofluids are envisioned to describe a fluid, in which nanometer-sized particles are annotated, in convectional heat transfer of basic fluids. Nanofluids are utilized in different engineering applications such as microelectronics, microfluidics, transportation, biomedical, solid-state lighting and manufacturing. Furthermore, suspensions of metal nanoparticles are also being developed for other purposes, such as medical applications including cancer therapy. Keblinski et al. [1] analyzed the case of possible mechanisms of enhancing thermal conductivity and he suggested that the size effect, the clustering of nanoparticles and the surface adsorption could be the major reason of enhancement, while the Brownian motion of nanoparticles contributes much less than other factors. This is because Brownian motion of nanoparticles is too slow to transport significant amount of heat through a nanofluid and this conclusion was also supported by their results of molecular dynamics simulation.

The nanofluid term point out to these kinds of fluids that created by immersing nanoscale particles in the base fluid, and the idea was presented by Choi [2]. Mahdy and Sameh [3] have calculated numerically laminar natural convective flow past a vertical wavy plate saturated porous medium of a nanofluid. The influence of thermophysical nanofluids' properties on the convective heat transfer and summarized various models used in the literature for portending the thermophysical nanofluids properties have been studied by Duangthongsuk and Wongwises [4]. Nield and Kuznetsov [5] reported the Cheng and Minkowycz problem [6] for natural convective boundary layer flow in a porous medium filled with nanofluid taking into account the combined influences of heat and mass transfer in the existing of thermophoresis and Brownian motion with considering Buongiorno model [7]. According to Lee et al. [8] and Eastman et al. [9] metallic nanoparticles enhance the thermal and electrical conductivity of the base fluid as well as the overall heat transfer rate compared to nonmetallic ones. They also observed that nanofluids' heat transfer rate becomes higher with increasing nanoparticle volume fraction. Khan and Pop [10] investigated the problem of natural nanofluid convection boundary layer flow past a horizontal flat plate embedded in a porous medium. Nanofluids have been shown to maximize the thermal conductivity and convective heat transfer performance of the base liquid by Abu-Nada [11]. Tiwari and Das [12] have proposed a theoretical model to analyze the nanofluids' behavior taking into account the solid volume fraction. Review papers [13]-[20] on convective heat transfer in nanofluids have been carried out for description of the characteristics of nanofluids in the past few years. In addition, a comprehensive survey of convective transport in nanofluids was made by Buongiorno [7]. Mixed convective heat and mass transfer flow is very important in manufacturing industries for the design of reliable equipment, nuclear plants, gas turbines and various propulsion devices for aircraft, missiles, satellites and space vehicles [21]-[25]. Besides, the phenomenon of bioconvection in nanofluid convection which is the aim of present contribution is driven by the presence of denser microorganisms accumulating on the surface of lighter water. The macroscopic convective motion of fluid caused by the density gradient is known as bioconvection and is created

A. Mahdy is with the South Valley University; Faculty of Science; Mathematics Department; Egypt (e-mail: mahdy@svu.edu.eg).

by collective swimming of motile microorganisms. These self-propelled motile microorganisms augment the density of the base fluid by swimming in a particular direction, thus causing bioconvection. Different bioconvection systems were studied on the basis of the mechanism of directional motion of the different types of microorganisms [26]-[33]. They focused on nanofluids containing gyrotactic microorganisms and reaffirm that the resultant large-scale motion of fluid caused by self-propelled motile microorganisms enhances mixing and prevent nanoparticle agglomeration in nanofluids. Unlike the motile microorganisms, the nanoparticles are not self-propelled, and their motion is driven by Brownian motion and thermophoresis occurring in the nanofluid. Thus, the motion of the motile microorganisms is independent of the motion of nanoparticles. A detailed discussion of bioconvection in suspensions of oxytactic bacteria is made for the onset of bioconvection in a suspension of gyrotactic/oxytactic microorganisms in different cases [34]-[37]. They performed stability analysis and determined the effect of small solid particles in a dilute suspension containing gyrotactic microorganisms, and introduced the concept of effective diffusivity to determine the effect of bioconvection on small solid particles. Mahdy [38], [39] analyzed the similarity and non-similarity solutions for Darcy free convection about an isothermal vertical cone with fixed apex half angle and wavy surface, pointing downwards in a nanofluid saturated porous medium contains gyrotactic microorganisms. Kuznetsov [40]-[42] made a series of analysis on a nanofluid bioconvection in a suspension containing both nanoparticles and microorganisms. He noticed that an adding of gyrotactic microorganisms inside nanofluids is likely to augment its stability as a suspension. He further detected that suspensions of gyrotactic microorganisms could exhibit bioconvection, which is a macroscopic motion in the fluid induced by up swimming or the motion of motile microorganisms. This is due to the fact that the motile microorganisms are usually heavier than water so that they can swim in the upward direction in response to stimuli such as gravity, light and chemical attractions. Regarding to the motivated literature review the objective of the present article is to analyze the behavior of microorganisms of mixed convection nanofluid flow over an isothermal vertical wedge saturated in a porous medium. Again, influences of Brownian motion and thermophoresis have been comprised for the nanofluid.

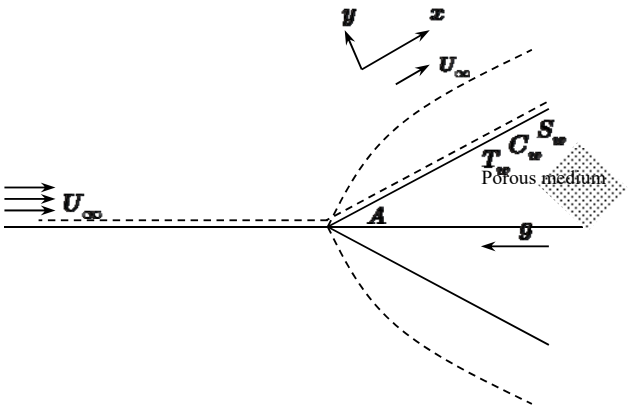

Fig. 1 Schematic diagram of physical model

II. Physical Configuration

In our article we take into consideration 2-dimensional boundary layer, steady state of mixed convection flow of optically dense viscous incompressible nanofluid fluid along an isothermal wedge of half angle A immersed in a saturated porous medium containing gyrotactic microorganisms. The physical paradigm and coordinate system is plotted in Fig. 1. The utilized nanofluid model combines the thermophoresis and Brownian motion influences. In addition, the temperature, the nanoparticle volume fraction and the density of motile microorganisms at the surface of wedge are constant and symbolized by T_w, C_w and S_w, respectively. The ambient values (at infinity) have been denoted, respectively, by T_∞, C_∞ and S_∞. The properties of the fluid have been assumed to be constant except for the density variations in the buoyancy force term. In addition, the nanoparticle suspension is considered to be stable, that is, nanoparticle agglomeration is ignored. Moreover, we ignore the effect of existing of nanoparticles on both of the direction of swimming microorganisms and on their swimming velocity. This is a reasonable assumption if the nanoparticle suspension is dilute (nanoparticle concentration is lower than 1%). Bioconvection induced flow only takes place in a dilute suspension of nanoparticles; otherwise, a large concentration of nanoparticles would result in a large suspension viscosity, which would restrain bioconvection. According to Oberbeck–Boussinesq approximation, the governing equations for the flow based on the Darcy's model within the boundary layer near the vertical wedge may be re-expressed as

$$\frac{\partial u}{\partial x}+\frac{\partial v}{\partial y}=0 \tag{1}$$

$$u = U_\infty + \frac{gK\cos A}{\mu}\begin{pmatrix}(1-C_\infty)\rho_{f\infty}\beta(T-T_\infty)\\ -(\rho_p-\rho_{f\infty})(C-C_\infty)\\ -\gamma(\rho_{m\infty}-\rho_\infty)(S-S_\infty)\end{pmatrix} \quad (2)$$

$$u\frac{\partial T}{\partial x}+v\frac{\partial T}{\partial y}=\alpha\frac{\partial^2 T}{\partial y^2}+\jmath\left(D\frac{\partial C}{\partial y}\frac{\partial T}{\partial y}+\frac{\tilde{D}}{T_\infty}\left(\frac{\partial T}{\partial y}\right)^2\right) \quad (3)$$

$$\epsilon^{-1}\left(u\frac{\partial C}{\partial x}+v\frac{\partial C}{\partial y}\right)=D\frac{\partial^2 C}{\partial y^2}+\frac{\tilde{D}}{T_\infty}\frac{\partial^2 T}{\partial y^2} \quad (4)$$

$$u\frac{\partial S}{\partial x}+v\frac{\partial S}{\partial y}+\frac{b\hat{W}}{C_w-C_\infty}\frac{\partial}{\partial y}\left(N\frac{\partial C}{\partial y}\right)=D_n\frac{\partial^2 S}{\partial y^2} \quad (5)$$

The boundary conditions for the problem at the wall of the wedge are presumed to be

$$\begin{aligned}&v(x,y)=0, \quad T(x,y)=T_w,\\ &C(x,y)=C_w,\ S(x,y)=S_w,\ y=0\end{aligned} \quad (6)$$

$$\begin{aligned}&u(x,y)\to U_\infty, \quad T(x,y)\to T_\infty,\\ &C(x,y)\to C_\infty, \quad S(x,y)\to S_\infty,\ y\to\infty\end{aligned} \quad (7)$$

In addition, the flow velocity potential for the wedge problem case may be re-formed as

$$U_\infty = ax^M, \qquad M=\frac{\lambda}{2-\lambda}$$

where a is a constant and λ indicates the Hartree pressure gradient parameter that corresponds to $\lambda = A\pi^{-1}$ for a total angle A of the wedge. In addition, u and v indicate the Darcy's velocity components along the x and y directions, μ is the dynamic viscosity of the fluid, α,β denote the thermal diffusivity and volumetric expansion coefficient, ρ_f is the density of the base fluid, ρ_p is the density of nanoparticles, $\rho_{m\infty}$ is the microorganism density, γ is the average volume of microorganisms; $\tilde{W}$ represents the constant maximum cell swimming speed, K is the Darcy permeability of the porous medium; ϵ is the porosity; $D,\tilde{D},D_n$ are the Brownian, thermophoretic diffusion and diffusivity of microorganisms coefficients, $\jmath=\epsilon(\rho c)_p\ /\ (\rho c)_f$ is the ratio of effective heat capacity of the nanoparticle material to the heat capacity of the fluid.

Upon the continuity equation, let us acquaint the stream function ψ which is defined by $u=\partial\psi\ /\ \partial y$, $v=-\partial\psi\ /\ \partial x$. So that (1) is satisfied identically. We are then left with the following four governing equations

$$\frac{\partial\psi}{\partial y}=\left(\frac{\partial\psi}{\partial y}\right)_\infty+\frac{gK\cos A}{\mu}\begin{pmatrix}(1-C_\infty)\rho_{f\infty}\beta(T-T_\infty)\\ -(\rho_p-\rho_{f\infty})(C-C_\infty)\\ -\gamma(\rho_{m\infty}-\rho_\infty)(S-S_\infty)\end{pmatrix} \quad (8)$$

$$\frac{\partial\psi}{\partial y}\frac{\partial T}{\partial x}-\frac{\partial\psi}{\partial x}\frac{\partial T}{\partial y}=\alpha\frac{\partial^2 T}{\partial y^2}+\jmath\left(D\frac{\partial C}{\partial y}\frac{\partial T}{\partial y}+\frac{\tilde{D}}{T_\infty}\left(\frac{\partial T}{\partial y}\right)^2\right) \quad (9)$$

$$\epsilon^{-1}\left(\frac{\partial\psi}{\partial y}\frac{\partial C}{\partial x}-\frac{\partial\psi}{\partial x}\frac{\partial C}{\partial y}\right)=D\frac{\partial^2 C}{\partial y^2}+\frac{\tilde{D}}{T_\infty}\frac{\partial^2 T}{\partial y^2} \quad (10)$$

$$\frac{\partial\psi}{\partial y}\frac{\partial S}{\partial x}-\frac{\partial\psi}{\partial x}\frac{\partial S}{\partial y}+\frac{b\hat{W}}{C_w-C_\infty}\frac{\partial}{\partial y}\left(S\frac{\partial C}{\partial y}\right)=D_n\frac{\partial^2 S}{\partial y^2} \quad (11)$$

Our review clarifies that most nanofluids have higher values of Lewis number Le. Because of this reason we focus on the case $Le>1$. As well as we suppose that mass transfer, rather than heat transfer, drives the flow. In terms of our model, this means that the buoyancy ratio parameter Nr (defined below) is smaller than unity. Again, this reveals that the Lewis number Le is greater than unity. It is more proper to mutate the governing equations into a case of dimensionless non-similar form that can be studied as an initial-value problem. For doing this let us acquaint the following non-similar transmutation:

$$\left.\begin{aligned}&\eta=\frac{y}{x\xi}Pe^{1/2}, \quad \xi=\left(1+\left(\frac{Ra}{Pe}\right)^{1/2}\right)^{-1},\\ &\psi=\alpha Pe^{1/2}\xi^{-1}f(\xi,\eta), \quad \theta(\xi,\eta)=\frac{T-T_\infty}{T_w-T_\infty},\\ &\phi(\xi,\eta)=\frac{C-C_\infty}{C_w-C_\infty}, \quad N(\xi,\eta)=\frac{S-S_\infty}{S_w-S_\infty},\\ &Pe=\frac{U_\infty x}{\alpha}\\ &Ra=\frac{(1-C_\infty)\rho_{f\infty}Kg\beta x(T_w-T_\infty)\cos A}{\mu\alpha},\end{aligned}\right\} \quad (12)$$

where the parameters Ra and Pe refer the Rayleigh and Peclet numbers. Upon the above transmutation, then the basic governing equations can be obtained in the form

$$f'=\xi^2+(1-\xi)^2\left(\theta-Nr\phi-Rb\,N\right) \quad (13)$$

$$\begin{aligned}&\theta''+\frac{1}{2}\left(1+M\xi\right)f\theta'+Nb\,\phi'\theta'+Nt\,\theta'^2=\\ &\frac{M}{2}\xi(1-\xi)\left(f'\frac{\partial\theta}{\partial\xi}-\theta'\frac{\partial f}{\partial\xi}\right)\end{aligned} \quad (14)$$

$$\phi'' + \frac{1}{2}\left(1 + M\xi\right) Le\, f\phi' + \frac{Nt}{Nb}\theta'' = \frac{M}{2}\xi(1-\xi)Le\left(f'\frac{\partial\phi}{\partial\xi} - \phi'\frac{\partial f}{\partial\xi}\right) \quad (15)$$

$$N'' + \frac{1}{2}\left(1 + M\xi\right) Lb\, fN' - Pb\left(N'\phi' + \phi''(N+\sigma)\right) = \frac{M}{2}\xi(1-\xi)Lb\left(f'\frac{\partial N}{\partial\xi} - N'\frac{\partial f}{\partial\xi}\right) \quad (16)$$

The dashes denote differentiation with respect to η. The converted dimensionless boundary conditions (6) and (7) are

$$(1+M\xi)f(\xi,0) = M\xi(\xi-1)\frac{\partial f(\xi,0)}{\partial\xi}, \quad \theta(\xi,0) = 1, \quad \phi(\xi,0) = 1, \quad S(\xi,0) = 1 \quad (17)$$

$$f'(\xi,\infty) \to \xi^2, \quad \theta(\xi,\infty) \to 0, \quad \phi(\xi,\infty) \to 0, \quad S(\xi,\infty) \to 0 \quad (18)$$

The parameter ξ denotes the mixed convection parameter and $\xi = 0\,(Pe = 0)$ coincides to the case of pure free convection and $\xi = 1\,(Ra = 0)$ coincides to the case of pure forced convection. The parameters Rb, Nr, Nb, Nt, Le, σ, Lb and Pb refer the bioconvection Rayleigh number, the buoyancy ratio, Brownian motion parameter, thermophoresis parameter, the Lewis number, the bioconvection constant, the bioconvection Lewis number and the bioconvection Péclet number, respectively and acquainted as

$$Rb = \frac{\gamma(\rho_{m\infty} - \rho_f)(N_w - N_\infty)}{\rho_{f\infty}\beta(1-C_\infty)(T_w - T_\infty)}, \quad Nr = \frac{(\rho_p - \rho_{f\infty})(C_w - C_\infty)}{\rho_{f\infty}\beta(1-C_\infty)(T_w - T_\infty)},$$

$$Nb = \frac{\epsilon D(\rho c)_p (C_w - C_\infty)}{(\rho c)_f \alpha}, \quad Nt = \frac{\epsilon\tilde{D}(\rho c)_p (T_w - T_\infty)}{(\rho c)_f \alpha T_\infty},$$

$$Le = \frac{\alpha}{\epsilon D}, \; L_b = \frac{\alpha}{D_n}, \; \sigma = \frac{N_\infty}{N_w - N_\infty}, \; Pb = \frac{b\hat{W}}{D_n}$$

The modified diffusivity ratio parameter is denoted by Nt (somewhat similar to the Soret parameter that arises in cross-diffusion phenomena), the parameter Le is the traditional Lewis number (the ratio of the Schmidt number to the Prandtl number).

The local density of the motile microorganisms Nn_x, the local Nusselt Nu_x and the local Sherwood Sh_x numbers are of particular importance for our investigation. These physical quantities can be acquainted as

$$Nu_x = \frac{xq_w}{k(T_w - T_\infty)} \quad (19)$$

$$Sh_x = \frac{xq_m}{D(C_w - C_\infty)} \quad (20)$$

$$Nn_x = \frac{xq_n}{D_n(N_w - N_\infty)} \quad (21)$$

respectively, q_w, q_m and q_n denote the wall heat, the wall mass and the wall motile microorganisms fluxes, and they are defined as

$$q_w = -k\frac{\partial T}{\partial y}\bigg|_{y=0}, q_m = -D\frac{\partial C}{\partial y}\bigg|_{y=0}, q_n = -D_n\frac{\partial N}{\partial y}\bigg|_{y=0} \quad (22)$$

Per those variables (12), (19)-(21) and (22), we obtain

$$\frac{Nu_x}{\sqrt{Pe} + \sqrt{Ra}} = -\theta'(\xi,0) \quad (23)$$

$$\frac{Sh_x}{\sqrt{Pe} + \sqrt{Ra}} = -\phi'(\xi,0) \quad (24)$$

$$\frac{Nn_x}{\sqrt{Pe} + \sqrt{Ra}} = -N'(\xi,0) \quad (25)$$

III. Results and Discussion

Now, the group of coupled non-linear ordinary differential equations (13)–(16) associated with its boundary conditions (17) and (18) have been solved numerically utilizing the method of an implicit finite difference scheme renowned as the Keller box method as illustrated by Cebeci and Bradshaw [43]. The computations were accomplished with $\Delta\xi = 0.01$ and $\Delta\eta = 0.01$ (uniform grids). The value of $\eta_\infty = 40$ is found to be sufficiently enough to obtain the accuracy of $|\theta'(0)| < 10^{-6}$. In addition, in order to confirm the numerical calculations, comparisons with the previously published results of Hsieh et al. [25], Yih [24] and Cheng [23] for the case of Newtonian fluid with $Rb = 0$ (absence of microorganisms) have been done. These comparisons are presented in Table I and it is observed that an excellent agreement has been found.

TABLE I
COMPARISON OF VALUES OF $-\theta'(\xi,0)$ FOR VARIOUS VALUES OF M AND ξ WITH ($Rb = Nr = Nb = Nt = 0$)

ξ	[23]	[25]	[24]	Present calculations				
	M = 0	M = 0	M = 0	M = 1/3	M = 1	M = 0	M = 1/3	M = 1
0.0	0.4438	0.4438	0.4437	0.4437	0.4437	0.4438	0.4438	0.4438
0.1	0.4036	0.4035	0.4035	0.4044	0.4049	0.4035	0.4044	0.4049
0.2	0.3733	0.3732	0.3732	0.3769	0.3786	0.3732	0.3769	0.3786
0.3	0.3551	0.3550	0.3550	0.3643	0.3697	0.3550	0.3643	0.3697
0.4	0.3506	0.3506	0.3505	0.3686	0.3823	0.3506	0.3686	0.3823
0.5	0.3603	0.3603	0.3603	0.3900	0.4227	0.3603	0.3900	0.4227
0.6	0.3833	0.3832	0.3832	0.4261	0.4854	0.3832	0.4261	0.4854
0.7	0.4174	0.4174	0.4173	0.4731	0.5599	0.4174	0.4731	0.5599
0.8	0.4603	0.4603	0.4602	0.5278	0.6385	0.4603	0.5278	0.6385
0.9	0.5098	0.5098	0.5097	0.5878	0.7181	0.5098	0.5878	0.7181
1.0	0.5642	0.5642	0.5642	0.6515	0.7979	0.5642	0.6515	0.7979

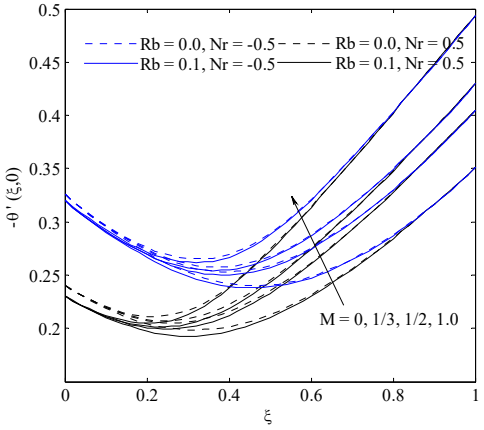

Fig. 2 Wedge angle parameter M effect on local Nusselt number

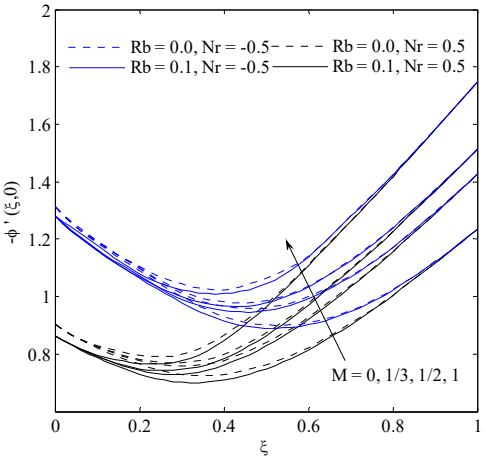

Fig. 3 Wedge angle parameter M effect on local Sherwood number

Because of the purpose of explaining the effects of such different governing parameters on the flow behavior near the wedge surface, numerical calculations have been achieved for various values of the governing parameters, namely; bioconvection Rayleigh number $0 \le Rb \le 0.5$ ($Rb = 0$ absent of microorganisms), mixed convection parameter $0 \le \xi \le 1.0$ ($\xi = 0$ coincides to the case of pure natural convection and $\xi = 1$ coincides to the case of pure forced convection.), bioconvection Lewis number $1 \le Lb \le 20$, bioconvection Peclet number $0.1 \le Pb \le 0.5$, buoyancy ratio parameter $-0.5 \le Nr \le 0.5$, traditional Lewis number $1 \le Le \le 10$, Brownian motion parameter $0.1 \le Nb \le 0.5$, thermophoresis parameter $0 \le Nt \le 1.0$ and wedge angle parameter $0 \le M \le 1$.

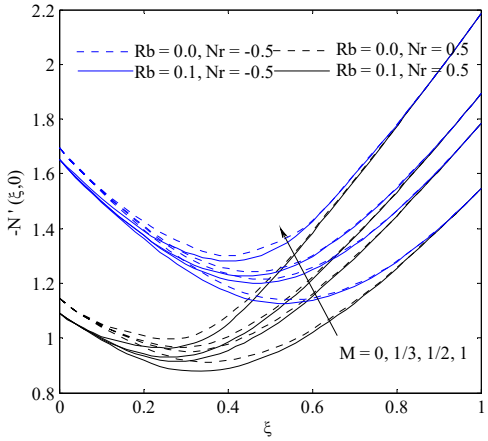

Fig. 4 Wedge angle parameter M effect on local density number of motile microorganisms

Figs. 2-4 illustrate the variation of the local Nusselt, Sherwood, density of motile microorganisms numbers, respectively with the mixed convection parameter ξ for various values of wedge angle parameter M according four cases namely, $Rb = 0$ and $Rb = 0.1$ and $Nr = -0.5, Nr = 0.5$. In addition the other parameter are chosen to be $Nb = Nt = 0.4$, $Le = Lb = 5.0$, $Pb = 0.3$, $\sigma = 0.1$, $M = 1/2$ and $\xi = 0.5$. It is clear that as the wedge angle parameter augmented, the local Nusselt number, local Sherwood number and local density of motile microorganisms number augment for forced convection and forced-convection-dominated mixed convection. The wedge angle parameter is frivolous for natural convection or natural-convection

dominated mixed convection.

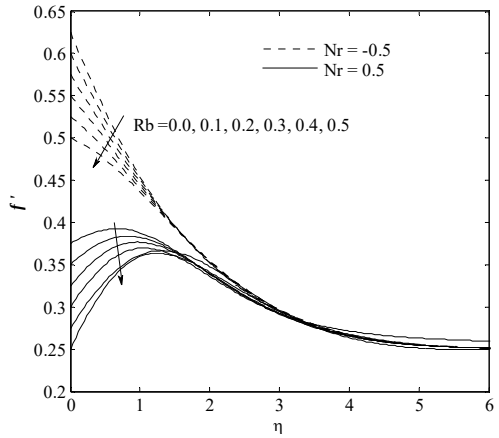

Fig. 5 Bioconvection Rayleigh number Rb effect on density velocity distribution

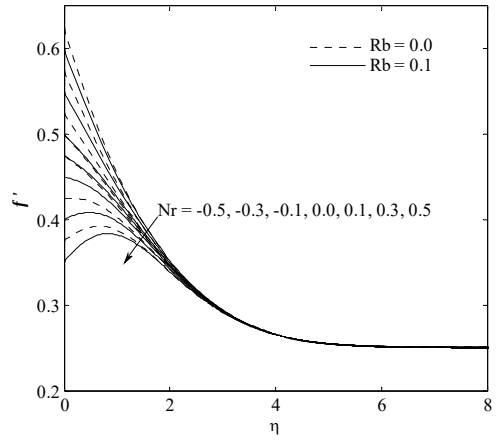

Fig. 6 Buoyancy ratio parameter Nr effect on velocity distribution

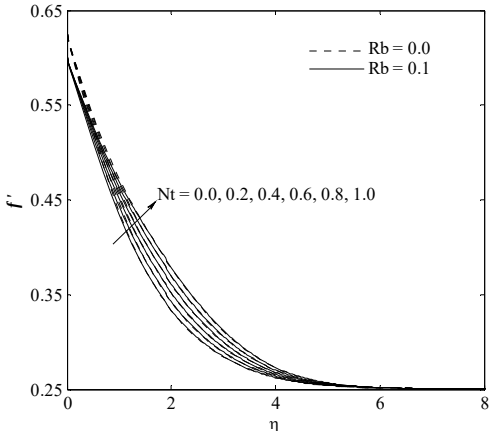

Fig. 7 Thermophoresis parameter Nt effect on velocity distribution

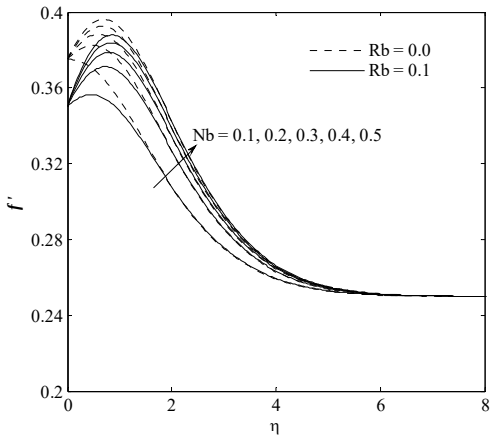

Fig. 8 Brownian motion parameter Nb effect on velocity distribution

Fig. 5 displays the variation of the dimensionless velocity profile for different values of bioconvection Rayleigh number Rb considering the two cases of buoyancy ratio $Nr = -0.5, Nr = 0.5$. In the case of absence of bioconvection, parameter $Rb = 0$, the non-dimensional velocity at the plate is detected to be higher. It can be observed that the non-dimensional velocity distribution minimizes with an augment in the buoyancy ratio (Fig. 6) and bioconvection Rayleigh number. The thermophoresis and Brownian motion parameter effects on velocity distribution are illustrated in Figs. 7 and 8 and it is observed that both of Brownian motion parameter and thermophoresis parameter tend to augment velocity distribution. The reason of this depends on the fact that the thermophoresis force (which tends to move particles from the hot to the cold zone) increases with an augment in Nt. In other words, the augment in the thermophoresis force maximizes the nanoparticle concentration. As $Nb = 0$, there is no additional thermal transport due to buoyancy effects created as a result of nanoparticle concentration gradients. It is noticed that the momentum boundary layer thickness augment with increasing values of Nb and Nt.

The Brownian motion parameter Nb can be described as the ratio of the nanoparticle diffusion (which is due to the Brownian motion effect) to the nanofluid thermal diffusion. Therefore, it is expected that the Brownian motion parameter increases with an increase in the difference between the nanoparticle volume fractions at the wall of the wedge and ambient. Based on the Einstein-Stokes equation [10], the Brownian motion is proportional to the inverse of the particle diameter. Hence, as the particle diameter decreases, the Brownian motion increases. Variation of the local Nusselt number, local Sherwood number and local density of motile microorganisms number with the mixed convection parameter for different values of Brownian motion parameter Nb are depicted in Figs. 9-11 when $Rb = 0, 0.1$ and $Nr = -0.5, 0.5$. It is clear that an increase in the Brownian motion parameter tends to minimize the local Nusselt number (Fig. 9) but augments both of the local Sherwood number (Fig. 10) and local density number of the motile microorganisms (Fig. 11).

Increasing the Brownian motion parameter tends to minimize the boundary-layer thickness of the nanoparticle volume fraction, thus augmenting the nanoparticle volume fraction gradient at the wall of the wedge. Brownian motion renders to warm the boundary layer and can enhance the thermal conductivity. For tiny particles, Brownian motion is strong and the parameter Nb will have high values and for large particles, Nb will have low values. Therefore, the Brownian motion can extend a significant enhancing effect on temperature distributions. Furthermore, Figs. 12-14 depict the effect of thermophoresis parameter Nt on the local Nusselt number, local Sherwood number and local density of the motile microorganisms number, against mixed convection variable ξ considering four cases namely, $R_b = 0.0, 0.1$ and $Nr = -0.5, 0.5$. The figures reveal that an augment in the thermophoresis parameter tends to minimize the local Nusselt and Sherwood numbers while maximizing the density number of the motile microorganisms.

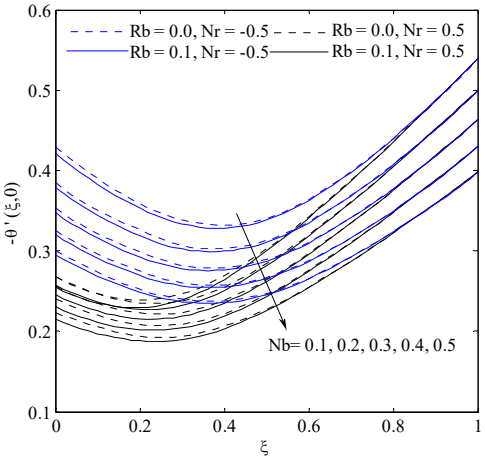

Fig. 9 Brownian motion parameter Nb effect on local Nusselt number

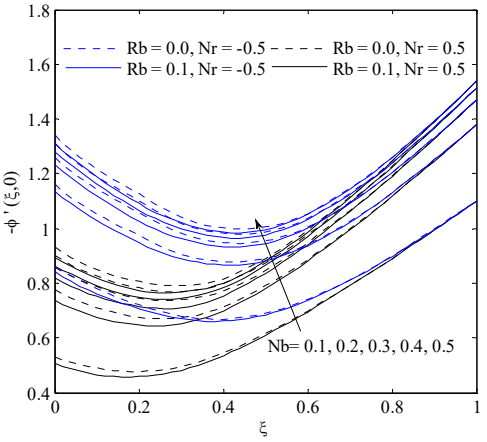

Fig. 10 Brownian motion parameter Nb on local Sherwood number

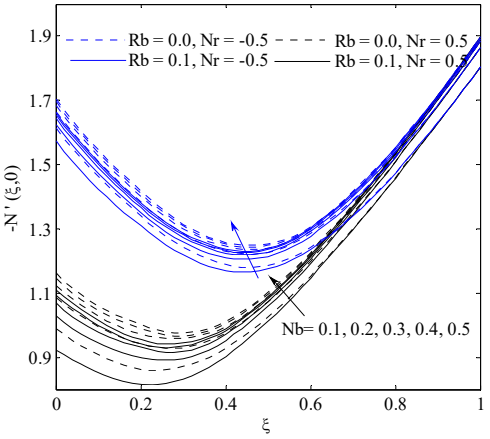

Fig. 11 Brownian motion parameter Nb effect on local density number of motile microorganisms

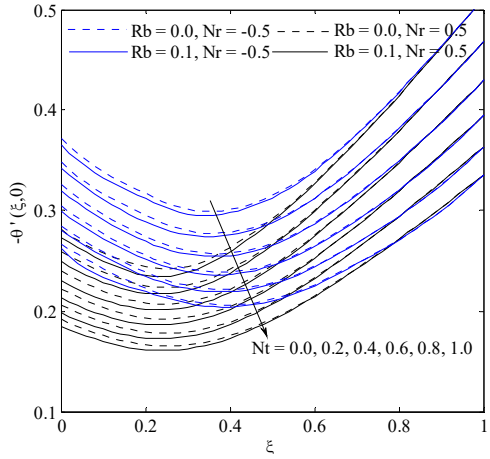

Fig. 12 Thermophoresis parameter Nt effect on local Nusselt number

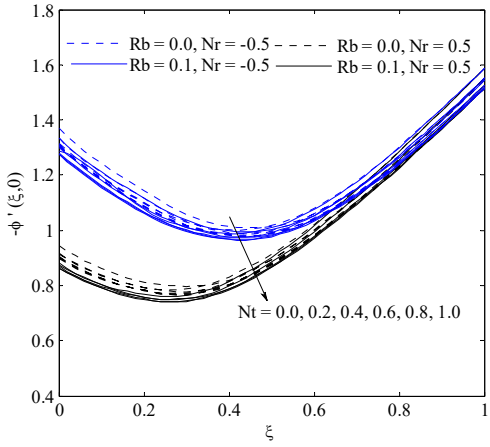

Fig. 13 Thermophoresis parameter Nt effect on local Sherwood number

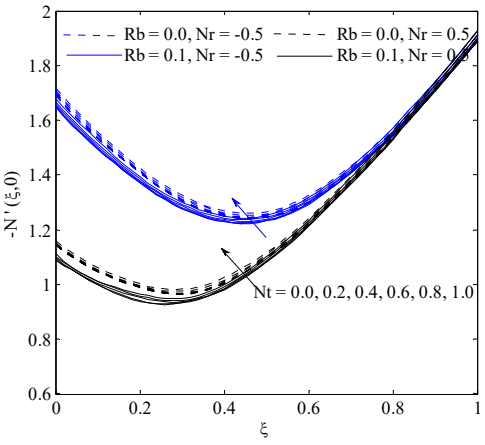

Fig. 14 Thermophoresis parameter Nt effect on local density number of motile microorganisms

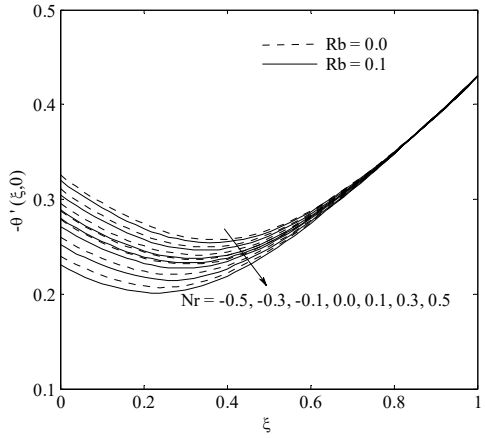

Fig. 15 Buoyancy ratio parameter Nr effect on local Nusselt number

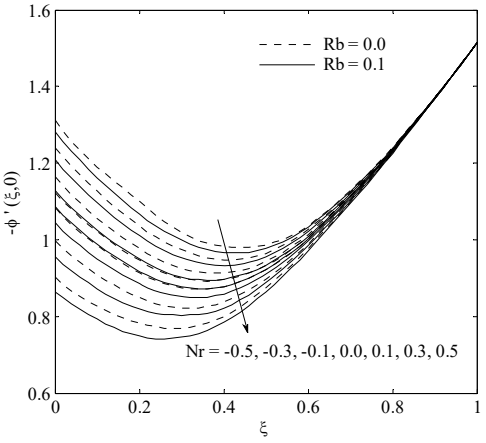

Fig. 16 Buoyancy ratio parameter Nr effect on local Sherwood number

Figs. 15-17 represent the variation of the local Nusselt number, local Sherwood number and local density number of motile microorganisms against mixed convection parameter for various values of buoyancy ratio parameter Nr when $Rb = 0, 0.1$. These figures display that as the buoyancy ratio parameter augments, all of Nu_x, Sh_x, Nn_x numbers minimize. However, for $\xi = 1$ (forced convection limit), the flow is uncoupled from the thermal and volume fraction buoyancy effects, and hence, there is no alteration in the local Nusselt, local Sherwood and local density motile of microorganisms numbers for all values of Nr. From the definition of ξ, it is seen that an augment in the value of the parameter Ra_x / Pe_x causes the mixed convection parameter ξ to minimize. Therefore, tiny values of Ra_x / Pe_x correspond to values of ξ close to unity, which indicate almost pure forced convection regime. On the other hand, elevation values of Ra_x / Pe_x correspond to values of ξ close to zero, indicating almost pure free convection regime. Moreover, equinoctial values of Ra_x / Pe_x represent values of ξ between 0 and 1, which correspond to the mixed convection regime.

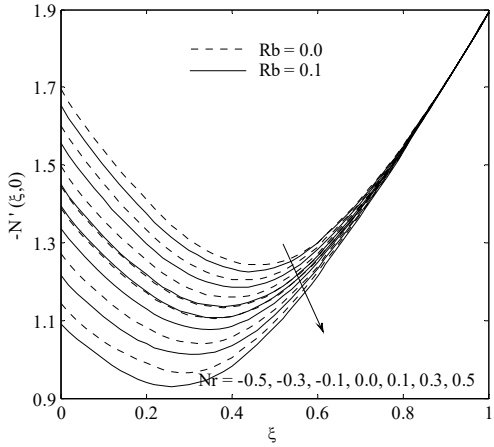

Fig. 17 Buoyancy ratio parameter Nr effect on local density number of motile microorganisms

Figs. 18-20 plotted the effect of bioconvection parameters, namely bioconvection Lewis number, bioconvection Peclet number and bioconvection Rayleigh number. From these figures we observe that the bioconvection Peclet Pb and bioconvection Lewis Lb numbers have the same effects. With increasing bioconvection Lewis or bioconvection Peclet numbers, the local density of motile microorganisms number increases, whereas it decreases with increase bioconvection Rayleigh number. The effect of bioconvection of Lewis number on density motile microorganisms is similar to Lewis number on nanoparticle concentration; that is, increasing bioconvection Lewis number tends to decrease the density motile microorganisms, Fig. 21. The effect of Lewis number on the local Sherwood number is illustrated in Fig. 22. Higher values of Lewis number lead to maximize the local Sherwood number. In fact, Brownian motion coefficient minimizes with rising transverse distance and due to this reason, the rescaled

nanoparticle volume fraction minimizes rapidly for large Lewis numbers. The last two figures, namely; Figs. 23 and 24 depict the effect of wedge angle parameter M on velocity and density motile microorganisms' distributions, it is observed that as M maximizes both of velocity and density motile microorganisms distributions minimize.

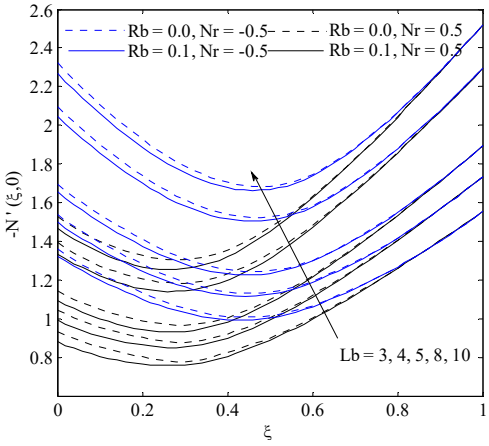

Fig. 18 Bioconvection Lewis number Lb effect on local density number of motile microorganisms

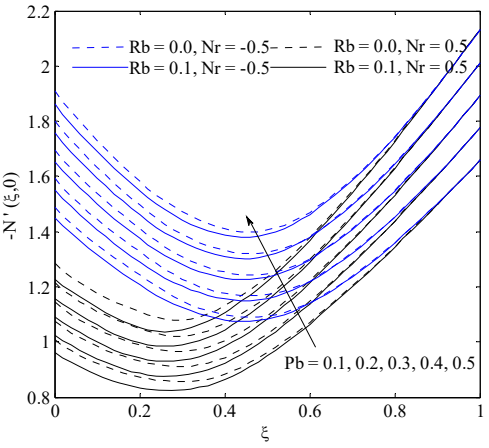

Fig. 19 Bioconvection Peclet number Pb effect on local density number of motile microorganisms

IV. Conclusion

Non-similarity-numerical approach is used to investigate the mixed convection boundary layer flow of a nanofluid over an isothermal vertical porous wedge containing gyrotactic microorganisms. By means of non-similarity reductions, a set of four coupled nonlinear equations with linear boundary conditions is obtained. This specific sort of nonlinear differential equations is solved numerically. Pertinent computations are illustrated graphically and discussed quantitatively with respect to variation in the controlling parameters. The dynamic impacts of nanoparticles, thermophoresis and Brownian motion, have been taken into regard in our nanofluid model. The wedge angle parameter is frivolous for natural convection or natural convection dominated mixed convection. The local density number of the motile microorganisms maximizes with an augment in Pb , M for forced convection and forced convection-dominated mixed convection and Lb but it minimizes with Rb.

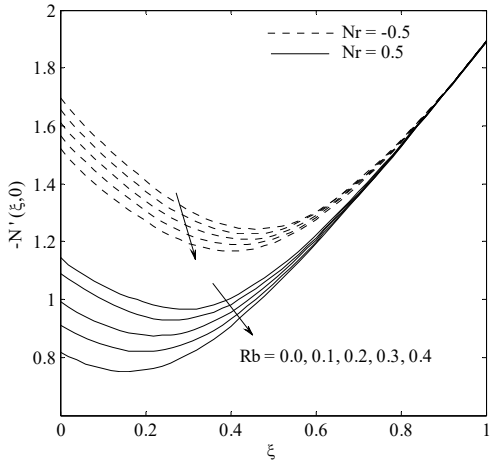

Fig. 20 Bioconvection Rayleigh number Rb effect on local density number of motile microorganisms

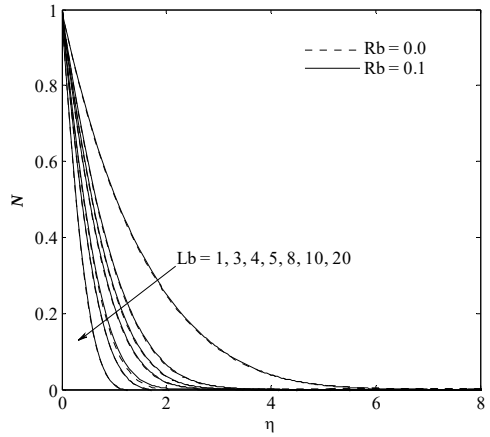

Fig. 21 Bioconvection Lewis number Lb effect on density of motile microorganisms

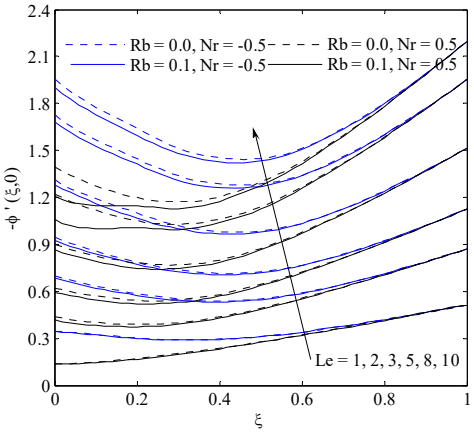

Fig. 22 Lewis number Le effect on local Sherwood number

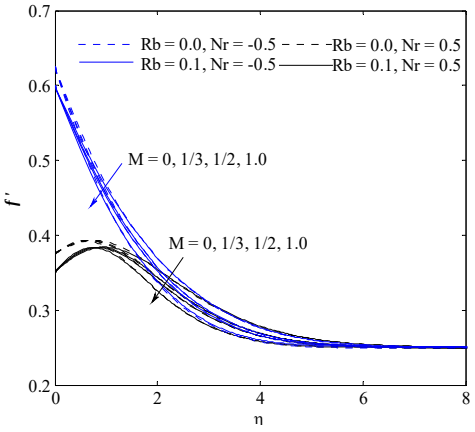

Fig. 23 Wedge angle parameter M effect on velocity distribution

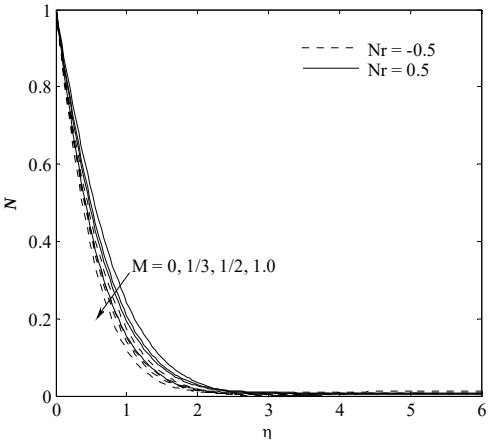

Fig. 24 Wedge angle parameter M effect on density of motile microorganisms

REFERENCES

[1] P. Keblinski, S.R. Phillpot, S.U.-S. Choi, J.A. Eastman, Mechanisms of heat flow in suspensions of nano-sized particles (nanofluids), Int. J. Heat Mass Transfer 45 (4) (2002) 855–863.

[2] U. S. U. Choi, Enhancing thermal conductivity of fluids with nanoparticle. In: Siginer, D.A., Wang H.P. (eds.), Developments and Applications of Non-Newtonian Flows, ASME FED, 231/MD 66 (1995) 99–105.

[3] A. Mahdy, S. E. Ahmed, Laminar free convection over a vertical wavy surface embedded in a porous medium saturated with a nanofluid. Transp. Porous Med. 91 (2012) 423–435.

[4] W. Duangthongsuk, S. Wongwises, Effect of thermophysical properties models on the predicting of the convective heat transfer coefficient for low concentration nanofluid. Int. Commun. Heat Mass Transf. 35 (2008) 1320–1326.

[5] D. A. Nield, A. V. Kuznetsov, The Cheng-Minkowycz problem for natural convective boundary layer flow in a porous medium saturated by a nanofluid. Int. J. Heat Mass Transf. 52 (2009) 5792-5795.

[6] P. Cheng, W. J. Minkowycz, Free convection about a vertical flat plate embedded in a porous medium with application to heat transfer from a dike. J. Geophys. Res. 28 (1977) 2040-2044.

[7] J. Buongiorno, Convective transport in nanofluids. ASME J. Heat Transf. 128 (2006) 240–250.

[8] S. Lee, S. U. S. Choi, S. Li, J. A. Eastman, Measuring thermal conductivity of fluids containing oxide nanoparticles. ASME J. Heat Transfer Trans (1999) 121-280.

[9] J. A. Eastman, S. U. S. Choi, S. Li, W. Yu, L. J. Thompson, Anomalously increased effective thermal conductivity of ethylene glycol-based nanofluids containing copper nanoparticles. Appl. Phys. Lett. 78 (2001) 718–720.

[10] W. A. Khan, I. Pop, Free convection boundary layer flow past a horizontal flat plate embedded in a porous medium filled with a nanofluid. ASME J. Heat Transf. 133 (2011) 094501-1.

[11] E. Abu-Nada, Application of nanofluids for heat transfer enhancement of separated flows encountered in a backward facing step, Int. J. Heat Fluid Flow 29 (2008) 242–249.

[12] R. K. Tiwari, M. K. Das, Heat transfer augmentation in a two-sided lid-driven differentially heated square cavity utilizing nanofluids. Int. J. Heat Mass Transf. 50 (2007) 2002-2018.

[13] S. Kakać, A. Pramuanjaroenkij, Review of convective heat transfer enhancement with nanofluids, Int. J. Heat Mass Transf. 52 (2009) 3187–3196.

[14] D. Wen, G. Lin, S. Vafaei, K. Zhang, Review of nanofluids for heat transfer applications, Particuology 7 (2011) 141–150.

[15] P. M. Congedo, S. Collura, Modeling and analysis of natural convection heat transfer in nanofluids. In: Proc ASME Summer Heat Transfer Conf. 3 (2009) 569–579.

[16] A. Chamkha, S. R. G. Rama, G. Kaustubh, Non-similar Solution for Natural Convective Boundary Layer Flow Over a Sphere Embedded in a Porous Medium Saturated with a Nanofluid. Transp. Porous Med. 86 (2011) 13–22.

[17] M. A. A. Hamad, I. Pop, A. I. Ismail, Magnetic field effects on free convection flow of a nanofluid past a semi-infinite vertical flat plate. Nonlinear Analysis: Real World Appl. 12 (2011) 1338–1346.

[18] D. A. Nield, A. V. Kuznetsov, Thermal instability in a porous medium layer saturated by a nanofluid: Brinkman model. Transp. Porous media 81 (2010) 409–422.

[19] Y. Xuan, W. Roetzel, Conceptions for heat transfer correlation of nanofluids. Int. J. Heat Mass Transf. 43 (2000) 3701-3707.

[20] A. J. Chamkha, A. M Aly, H. Al-Mudhaf, Laminar MHD mixed convection flow of a nanofluid along a stretching permeable surface in the presence of heat generation or absorption effects. Int. J. Microscale Nanoscale Thermal Fluid Transp. Phenom. 2 (2011).

[21] M. Kumari, G. Nath, Radiation effect on mixed convection from a horizontal surface in a porous medium. Mech. Res. Commun. 31 (2004) 483–491.

[22] D. A. Nield, A. Bejan, Convection in Porous Media. 2nd edn. Springer, New York (2006).

[23] C-Y. Cheng, Soret Dufour effects on mixed convection heat and mass transfer from a vertical wedge in a porous medium with constant wall temperature and concentration, Transp. Porous Med. 94 (2012) 123-132.

[24] K. A. Yih, Radiation effect on mixed convection over an isothermal wedge in porous media: the entire regime. Heat Transf. Eng. 22 (2001) 26–32.

[25] J. C. Hsieh, T. S. Chen, B. F. Armaly, Mixed convection along a non-isothermal vertical plate embedded in a porous medium: the entire regime. Int. J. Heat Mass Transf. 36 (1993) 1819–1825.

[26] P. Geng, A. V. Kuznetsov, Settling of bidispersed small solid particles in a dilute suspension containing gyrotactic microorganisms. Int. J. Eng. Sci. 43 (2005) 992-1010.

[27] P. Geng, A. V. Kuznetsov, Effect of small solid particles on the development of bioconvection plumes. Int. Commun. Heat Mass Transfer 31 (2004) 629-638.

[28] P. Geng, A. V. Kuznetsov, Introducing the concept of effective diffusivity to evaluate the effect of bioconvection on small solid particles. Int. J. Transp. Phenom. 7 (1995) 321–338.

[29] W. A. Khan, M. J. Uddin, A. I. Ismail, Free convection of non-Newtonian nanofluids in porous media with gyrotactic microorganisms. Transp Porous Med. 97 (2013) 241–252.

[30] A. J. Hillesdon, T. j. Pedley, Bioconvection in suspensions of oxytactic bacteria: linear theory. J. Fluid Mech. 324 (1996) 223-259.

[31] A. Aziz, W. a. Khan, I. Pop, Free convection boundary layer flow past a horizontal flat plate embedded in porous medium filled by nanofluid containing gyrotactic microorganisms. Int. J. Thermal Sci. 56 (2012) 48–57.

[32] S. M. Becker, A. V. Kuznetsov, A. A. Avramenko, Numerical modeling of a falling bioconvection plume in a porous medium. Fluid Dyn. Res. 33 (2004) 323-339.

[33] W. N. Mutuku, O. D. Makinde, Hydromagnetic bioconvection of nanofluid over a permeable vertical plate due to gyrotactic microorganisms. Computers & Fluids 95 (2014) 88–97.

[34] S. Childress, M. Levandowsky, E. A. Spiegel, Pattern formation in a suspension of swimming microorganisms – equations and stability

theory. J. Fluid Mech. 69 (1975) 591–613.
[35] A. A. Avramenko, A. V. Kuznetsov, Stability of a suspension of gyrotactic microorganisms in superimposed fluid and porous layers. Int. Commun. Heat Mass Transfer 31 (2004) 1057–1066.
[36] A. V. Kuznetsov, The onset of nanofluid bioconvection in a suspension containing both nanoparticles and gyrotactic microorganisms. Int. Commun. Heat Mass Transf. 37 (2010) 1421–1425.
[37] W. A. Khan, O. D. Makinde, Z. H. Khan, MHD boundary layer flow of a nanofluid containing gyrotactic microorganisms past a vertical plate with Navier slip. Int. J. Heat Mass Transf. 74 (2014) 285–291.
[38] A. Mahdy, Natural convection boundary layer flow due to gyrotactic microorganisms about a vertical cone in porous media saturated by a nanofluid. J. Braz. Soc. Mech. Sci. Eng. 38 (2016) 67-76.
[39] S. E. Ahmed, A. Mahdy, Laminar MHD natural convection of nanofluid containing gyrotactic microorganisms over vertical wavy surface saturated non-Darcian porous media, Applied Mathematics and Mechanics 37 (2016) 471-484.
[40] A. V. Kuznetsov, The onset of thermo-bioconvection in a shallow fluid saturated porous layer heated from below in a suspension of oxytactic microorganisms. Eur. J. Mech. – B/Fluids 25 (2006) 223–233.
[41] A. V. Kuznetsov, Bio-thermal convection induced by two different species of microorganisms. Int. Commun. Heat Mass Transf. 38 (2011) 548–553.
[42] A. V. Kuznetsov, Nanofluid bioconvection in water-based suspensions containing nanoparticles and oxytactic microorganisms: oscillatory instability. Nanoscale Res. Lett. 6 (2011) 1-13.
[43] T. Cebeci, P. Bradshaw, Physical and computational aspects of convective heat transfer, Berlin-Heidelberg-New york- Springer-Verlag (1984).